

Guidelines on wave overtopping discharges at rubble mound breakwaters including slope angle effects

Marcel R.A. van Gent¹, Jaap van Marrewijk² and Patricia Mares-Nasarre³

Abstract

Mean wave overtopping discharges at rubble mound breakwaters were measured in a wave flume for various rock-armoured slopes. In the physical model tests, the structure slope was varied: 1:1.5, 1:2, 1:4, 1:6 and 1:8 slopes were studied. The mean wave overtopping discharges appeared to be strongly dependent on the structure slope for both “breaking waves” and for “non-breaking waves”. Existing expressions that also account for friction, a berm (if present), a protruding crest wall (if present), and the angle of wave attack, were extended by incorporating both the slope angle and the wave steepness of the incident waves at the toe. The match between the empirical equations and the data (new and earlier tests) is good. The guidelines to estimate wave overtopping discharges as presented here perform much better than existing guidelines since most existing guidelines for rubble mound breakwaters ignore the explicit influence of the structure slope and the wave steepness. Both for “breaking waves” and for “non-breaking waves”, the structure slope and the wave steepness clearly affect wave overtopping discharges, and therefore expressions that ignore these effects should not be used if accurate estimates of mean wave overtopping discharges are required.

Keywords


Wave overtopping, Coastal structures, Rubble mound breakwaters, Discharges, Slope angle, Shallow water, Crest walls, Berms, Roughness, Wind, Oblique waves, Wave flume tests, Guidelines

¹ Marcel.vanGent@deltares.nl; Deltares and Delft University of Technology, Delft, The Netherlands
² Jaap.vanMarrewijk@sweco.nl; Delft University of Technology, presently at SWECO, The Netherlands
³ P.MaresNasarre@tudelft.nl; Delft University of Technology, Delft, The Netherlands

Research Article. **Submitted:** April 17th, 2025. **Reviewed:** June 10th, 2025. **Accepted** after double-anonymous review: July 10th, 2025. **Published:** September 3rd, 2025.

DOI: <http://doi.org/10.59490/jchs.2025.0048>

Cite as: “Van Gent, M. R., van Marrewijk, J., & Mares-Nasarre, P. Guidelines on wave overtopping discharges at rubble mound breakwaters including slope angle effects. *Journal of Coastal and Hydraulic Structures*. <https://doi.org/10.59490/jchs.2025.0048>”

The Journal of Coastal and Hydraulic Structures is a community-based, free, and open access journal for the dissemination of high-quality knowledge on the engineering science of coastal and hydraulic structures. This paper has been written and reviewed with care. However, the authors and the journal do not accept any liability which might arise from use of its contents. Copyright ©2025 by the authors. This journal paper is published under a CC-BY-4.0 license, which allows anyone to redistribute, mix and adapt, as long as credit is given to the authors. 

ISSN: 2667-047X online

1 Introduction

For the design and adaptation of rubble mound breakwaters, accurate wave overtopping estimates are important to determine the required crest level. To characterize potential threats due to wave overtopping, mean wave overtopping discharges during the peak of a storm are generally used, although parameters describing individual wave overtopping events are also valuable. Estimates of wave overtopping discharges are not only relevant for the design, but also for existing structures that require adaptation due to sea level rise and its potential effects on the wave loading. Adaptation

of existing structures can include adding a berm, adding a crest wall, adding a low-crested structure in front of the breakwater, increasing the foreshore in front of the structure, or modifying the seaward slope to a milder slope.

Estimates of wave overtopping discharges are generally based on physical modelling in wave flumes and wave basins, or on empirical equations based on such tests. However, also numerical modelling of wave overtopping at coastal structures can be used to estimate wave overtopping parameters, see for instance Chen *et al.* (2021, 2022), Jin *et al.* (2022), Irías Mata and Van Gent (2023) and Stagnitti *et al.* (2023). Numerical modelling can be used in combination with physical modelling by studying the influence of parameters over a wider range than those applied in physical model tests. Existing empirical expressions for overtopping discharges are available in manuals such as TAW (2002) and EurOtop (2018). However, these guidelines are outdated for estimates of mean wave overtopping discharges at rubble mound breakwater due to new knowledge. This includes insights into for instance the influence of shallow foreshores (*e.g.* De Ridder *et al.*, 2024), the configuration of a berm in the seaward slope or a crest wall on top of the structure (*e.g.* Van Gent *et al.*, 2022), the influence of roughness (*e.g.* Eldrup *et al.*, 2022; Pepi *et al.*, 2022), oblique wave attack (*e.g.* Van Gent, 2024), or a second wave field in addition to the primary wave field (*e.g.* Van der Werf and Van Gent, 2018; Vieira Leite *et al.*, 2019). However, in these studies no systematic variation was performed for the slope angle of the structure. For so-called “breaking waves” on the slope of dikes the influence of the slope is clear, and present in empirical expressions. However, the influence of the structure slope is not explicitly present in expressions for rubble mound breakwaters, neither for “breaking waves” on the slope nor for “non-breaking waves” (see for instance EurOtop, 2018; Eq.6.5). In any case, in these studies no systematic variation of the slope over a wide range of slopes within the same test set-up, has been performed. Such tests can provide quantitative information on the influence of the slope angle, in addition to clear indications (see for instance Irías Mata and Van Gent, 2023) that the slope angle not only affects the mean wave overtopping discharges for “breaking waves” but also for “non-breaking waves”. EurOtop (2018), Eldrup *et al.* (2022) and Pepi *et al.* (2022) include the influence of the slope angle and wave steepness in an expression for the roughness. However, for equal roughness (for instance, for the extreme case of “no roughness”) there is no influence of the slope angle according to these expressions. Here, the explicit influence of the slope angle is studied and incorporated in expressions for the mean wave overtopping discharge at statically stable rubble mound breakwaters with a permeable core. The contribution of this research is threefold:

- 1) What is the influence of the slope angle of rock-armoured rubble mound structures on mean wave overtopping discharges?
- 2) How can the effects of the slope angle, freeboard, wave height, wave steepness, oblique waves, roughness, a berm in the seaward slope, a protruding crest wall, and the influence of wind be incorporated in empirical equations to estimate wave overtopping discharges at rock-armoured rubble mound structures?
- 3) How do the derived empirical expressions to estimate overtopping discharges perform for other datasets including data obtained with severe wave breaking at the shallow foreshore?

To answer these research questions, physical model tests have been performed in a wave flume at Deltares, Delft. The paper is presented in five main sections. First, wave overtopping is discussed further in Section 2. The physical model tests are described and analysed in Section 3. Section 4 provides a discussion, while the conclusions and recommendations are described in Section 5.

2 Wave overtopping

Wave overtopping at coastal structures can be characterised by mean wave overtopping discharges during the peak of a storm or by parameters characterising overtopping events such as overtopping volumes per wave, flow velocities and flow depths. In the present study, mean wave overtopping discharges at rubble mound breakwaters are addressed. Important initial research with respect to mean wave overtopping discharges is described in Goda (1971), Battjes (1974) and Owen (1980). Thereafter, various formulas have been developed to predict wave overtopping at statically stable rubble mound breakwaters. Many can be rewritten as follows:

$$\frac{q}{\sqrt{gH_{m0}^3}} = a \exp \left[-\frac{b}{\gamma} \left(\frac{R_c}{H_{m0}} \right)^c \right] \quad (1)$$

where q is the mean wave overtopping discharge ($\text{m}^3/\text{s}/\text{m}$), g is the acceleration due to gravity (m/s^2), H_{m0} is the spectral significant wave height of the incident waves at the toe of the structure (m), R_c is the crest freeboard relative to the still water level (m), and γ denotes influence factors (-). $Q=q^*=q/(gH_{m0}^3)^{0.5}$ is the non-dimensional wave overtopping discharge. For the coefficient c many studies used $c=1$. EurOtop (2018) used $c=1.3$, while Gallach-Sánchez (2018) and Gallach-Sánchez *et al.* (2021) proposed $c=1.1$. If, unlike in Eq.1, the influence factor γ were to be used to a power c , as applied in EurOtop (2018), the value of the influence factor γ needs to be modified if c is unequal to one.

For relatively mild structure slopes, wave conditions often lead to plunging waves on the seaward slope (“breaking waves”), while for relatively steeper slopes wave conditions often lead to surging waves (“non-breaking waves”). For dikes that often have a relatively mild slope compared to many rubble mound breakwaters, wave overtopping expressions for plunging waves are often used with an expression for surging waves serving as an upper limit (see for instance TAW, 2002). For rubble mound breakwaters with relatively steep slopes, often only a wave overtopping expression for surging waves is applied (see for instance EurOtop, 2018; Eq.6.5).

Existing expressions for plunging waves on coastal structures such as dikes contain an influence of the slope of the structure, the wave steepness, a berm (if present), a protruding crest wall (if present) and other influence factors such as roughness and oblique wave attack (*e.g.* TAW, 2002). For surging waves some available expressions such as the one proposed by EurOtop (2018; Eq.6.5) contain no explicit influence of the slope of the structure, the wave steepness, a statically stable berm (if present), and a protruding crest wall (if present). Since all of these parameters affect wave overtopping discharges (*e.g.* Lioutas *et al.*, 2012; Molines and Medina, 2015; Medina and Molines, 2016); Koosheh *et al.*, 2022; Van Gent *et al.*, 2022; Irías Mata and Van Gent, 2023) also for surging waves, the expression proposed by EurOtop (2018; Eq.6.5) is insufficient and has been improved in several studies. In the present study the focus of new physical model tests is on including effects of the slope angle, not only for plunging waves but also for surging waves.

Besides effects of the structure slope, the wave steepness, a berm and a protruding crest element, also the roughness of the slope, the presence of swell in combination with wind waves, and wind itself, affect wave overtopping. For guidance on the effects of statically stable berms and crest walls reference is made to Van Gent *et al.* (2022). The reducing effect of a berm depends on the vertical position of the berm, the width of the berm and the wave steepness (see also Eq.4). The influence of the protruding part of the crest wall depends on the ratio of the height of the protruding part of the crest wall and the freeboard (see also Eq.5).

For guidance on the effects of roughness of rock armour layers with a layer thickness of about two diameters, reference is made to Bruce *et al.* (2009), Molines and Medina (2015), Medina and Molines (2016), Eldrup and Lykke Andersen (2018), EurOtop (2018) and Van Gent *et al.* (2022). Constant roughness influence factors have been proposed, often in the range of $\gamma_r=0.4$ to 0.5 . EurOtop (2018; Eq.6.7) proposed a constant roughness for lower values of the surf-similarity parameters ($\xi_{m-1,0} = \tan \alpha / s_{m-1,0}^{0.5}$ where the wave steepness $s_{m-1,0} = 2\pi H_{m0} / (gT_{m-1,0}^2)$ is based on the spectral wave period $T_{m-1,0}$), and a reduced influence of the roughness for higher values of the surf-similarity parameter. In Van Gent *et al.* (2022) an expression is proposed where the roughness depends on the size of the stones in the armour layer (Eq.3).

For guidance on the effects of low-frequency waves or swell in combination with wind waves reference is made to Van der Werf and Van Gent (2018). The presence of low-frequency waves or swell in combination with wind waves can be accounted for by virtually lowering the freeboard with about half of the wave height of the low-frequency waves or swell ($H_{m0\text{-swell}}$), see also Eq.2.

For guidance on the effects of oblique waves on wave overtopping at rubble mound structures reference is made to Van Gent and Van der Werf (2019) and Van Gent (2022), see also Eq.6.

For the power c in Eq.1, various values have been proposed but no clear evidence that a value other than $c=1$ would perform better for rubble mound breakwaters is available (see also Van Gent *et al.*, 2022), so here the power $c=1$ is used in Eq.1. For “breaking waves” on the structure slope, empirical expressions exist (*e.g.* TAW, 2002) where the influence of the slope angle and wave steepness have partly been taken into account by using the surf-similarity parameter in the exponential part of the expression, while the remaining influences of the slope angle and wave steepness are taken into account in expressions for a . In the following Eq.2 is used with influence factors for friction, a berm, a protruding crest wall, and oblique waves. Thus, in Eq.2 a can depend on the slope angle and wave steepness, while the values for b and c (the power c for the surf-similarity in Eq.2) depend on whether the conditions can be considered as “breaking waves” or “non-breaking waves”. These dependencies are subject of the present study. The following set of expressions is used:

$$q^* = \frac{q}{\sqrt{gH_{m0}^3}} = a \exp \left[-b \frac{R_c - c_{swell} H_{m0-swell}}{\gamma_f \gamma_b \gamma_v \gamma_\beta (\xi_{m-1,0})^c H_{m0}} \right] \quad (2)$$

with

$$\text{Friction:} \quad \gamma_f = 1 - c_{f1} \left(\frac{D_{n50}}{H_{m0}} \right)^{c_{f2}} \quad (3)$$

$$\text{Berm:} \quad \gamma_b = 1 - c_{b1} \left(\frac{s_{m-1,0} B}{H_{m0}} \right)^{c_{b2}} \left(1 - c_{b3} \left(\frac{B_L}{s_{m-1,0} A_c} \right)^{c_{b4}} \right) \quad (4)$$

$$\text{Protruding crest wall:} \quad \gamma_v = 1 + c_v \left(\frac{R_c - A_c}{R_c} \right) \quad (5)$$

$$\text{Oblique waves:} \quad \gamma_\beta = (1 - c_\beta) \cos^2 \beta + c_\beta \quad (6)$$

where q^* is the non-dimensional overtopping discharge, H_{m0} is the spectral significant wave height of the incident waves at the toe of the structure (m), R_c is the freeboard relative to the still water level (m), $H_{m0-swell}$ is the spectral significant wave height of a second wave field of long waves such as infragravity waves or swell (for instance from a different direction), if present (m), $\xi_{m-1,0}$ is the surf-similarity parameter (Iribarren number), D_{n50} is the stone diameter of the stones in the armour layer (m), B is the berm width (m), A_c is the level of the crest of the armour layer relative to the still water level (m), B_L is the vertical distance of the berm relative to the crest of the armour A_c (m), and β is the angle of wave attack ($\beta=0^\circ$ for perpendicular wave attack). Based on earlier research (Van Gent and Van der Werf, 2019; Van Gent, 2022; Van Gent *et al.*, 2022) the coefficients $c_{f1}=0.7$, $c_{f2}=0.1$, $c_{b1}=18$, $c_{b2}=1.3$, $c_{b3}=0.34$, $c_{b4}=0.2$, $c_v=0.45$, $c_\beta=0.35$, and $c_{swell}=0.4$ have been obtained for rubble mound breakwaters.

The influence of wind on wave overtopping at structures with a protruding crest wall depends on the magnitude of the wave overtopping discharge itself. The effect of wind can be accounted by using the following expression in the case of perpendicular wave attack (Van Gent *et al.*, 2024):

$$\text{Overtopping with wind:} \quad q_w = \gamma_w q \quad \text{with} \quad \gamma_w = 1 + c_{w1} \frac{h_c}{H_{m0}} (q^*)^{c_{w2}} \quad (7)$$

where q_w is the overtopping discharge including effects of onshore wind, q is the overtopping discharge without effects of wind (for instance obtained using Eq.2), and h_c is the protruding part of the crest wall ($h_c = R_c - A_c$). Note that $q_w = \gamma_w q$ is equal to $q_w^* = \gamma_w q^*$ since both discharges (q_w^* and q^*) are made non-dimensional with the same wave height. Based on earlier research (Van Gent *et al.*, 2024), the coefficients $c_{w1}=0.075$ and $c_{w2}=-0.3$ have been determined.

The new tests in the present study are with structures without a berm ($\gamma_b=1$) and without a protruding crest wall ($\gamma_v=1$), for perpendicular wave attack ($\gamma_\beta=1$), without effects of wind ($\gamma_w=1$), and for sea states without a second wave field from another direction ($H_{m0-swell}=0$).

The described expressions (Eqs.1-7) were derived based on conditions without severe wave breaking on the foreshore. For effects of shallow foreshores on wave overtopping at rubble mound structures, reference is made to De Ridder *et al.* (2024, 2025). Although the new tests for various slope angles are for conditions without severe wave breaking on the foreshore, the comparison with test results by De Ridder *et al.* (2024) is described.

3 Physical model tests

3.1 Test programme

The physical model tests were performed in a 55 m long section of the Scheldt Flume (110 m long, 1 m wide, and 1.2 m high) at Deltares, Delft. The tests are described in detail in Van Marrewijk (2024). The wave generator is equipped with active reflection compensation, accounting for short-waves and long-waves reflection. This means that the motion of the wave paddle compensates for the waves reflected by the structure, preventing them from being re-reflected at the wave paddle and propagating towards the model. Second-order wave generation was applied. Wave gauges were positioned at the horizontal foreshore to separate incident and reflected waves from the measured surface elevations

(based on Zelt and Skjelbreia, 1992, and De Ridder *et al.*, 2023); one set of seven wave gauges was positioned about 9 m from the wave generator and another set of seven wave gauges was positioned closer to the toe of the structures at 14 m from the wave generator, with the closest wave gauge at a distance 0.40 m from the toe.

Five rubble mound structures with a permeable core were tested where the seaward slope was varied: 1:1.5, 1:2, 1:4, 1:6 and 1:8. The rest of the structure configurations remained the same. The crest height was 0.900 m above the bottom of the flume. All structures consisted of an armour layer with a thickness of $d_a=0.060$ m, a stone diameter of $D_{n50}=0.0317$ m, an underlayer with a thickness of $d_u=0.030$ m and a stone diameter of $D_{n50}=0.0168$ m, and a permeable core with a stone diameter of $D_{n50}=0.0065$ m. At the crest, on top of the core, a non-protruding crest wall with a total width of 0.140 m was placed at $G_c=0.100$ m from the start of the armour at the crest (see Figure 1). No recurved parapet (bullnose) was applied on the crest wall. The rear side slope was 1:1.5. An overtopping chute was placed between the tip of the crest wall and the overtopping box. Stones were fixed such that no displacements of stones occurred. The upper part of the seaward slope (1.35 m) up to the transition to the horizontal crest was placed on a frame that was reused for each of the five slopes. This not only prevented potential movements of stones that could affect wave overtopping but also ensured that the orientation of the stones and permeability of the armour layer in the upper part of the slope was equal for each of the five slopes. A sketch of the structure with a 1:2 slope is shown in Figure 1.

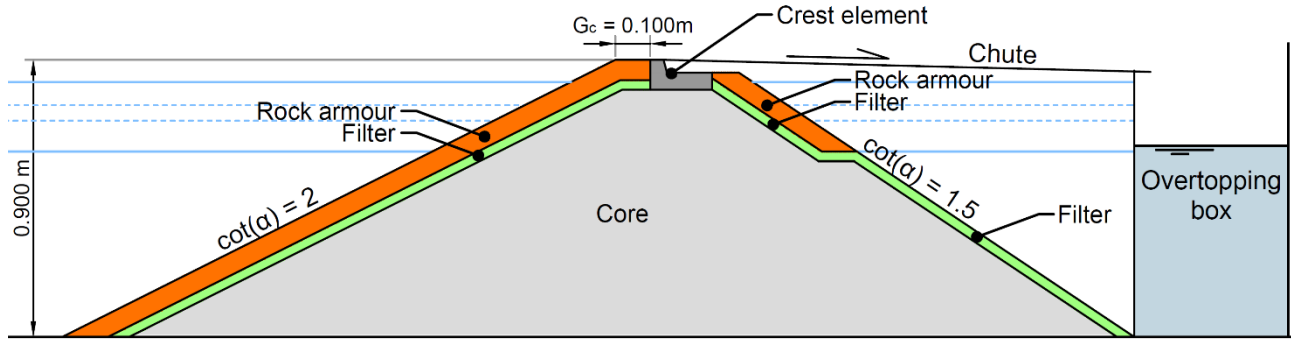


Figure 1: Sketch of the cross-section of the rubble mound structure with a 1:2 seaward slope.

In all tests a JONSWAP wave spectrum was used (with the standard peak enhancement factor of 3.3). All tests consisted of about 1000 waves. Tests were performed with incident significant wave heights between $H_{m0}=0.096$ m and 0.228 m (for all slopes). Three values of the wave steepness were used, leading to a wave steepness between $s_{m-1,0}=0.012$ and 0.042 ($s_{m-1,0}=2\pi H_{m0}/(gT_{m-1,0}^2)$). Use is made of the spectral mean period $T_{m-1,0}$ since this wave period describes the influence of the spectral shape on for instance wave run-up, wave overtopping, and wave reflection at coastal structures (see Van Gent, 1999, 2001, and Dekker *et al.*, 2007). The surf-similarity parameter (Iribarren number) $\xi_{m-1,0}=\tan \alpha / s_{m-1,0}^{0.5}$ varied between 0.612 and 6.04. Four water depths were applied (*i.e.* 0.600 m, 0.700 m, 0.750 m and 0.825 m), leading to various levels of the freeboard (R_c). The non-dimensional freeboard was in the range between $0.33 \leq R_c / H_{m0} \leq 2.08$. In total, 120 tests resulted in wave overtopping. Table 1 shows the ranges of the most important parameters of the test programme. Figure 2 shows pictures of wave action on various slopes.

Table 1: Parameter ranges of the test programme.

Parameter	Symbol	Values/Ranges
Seaward slope (-)	$\cot \alpha$	1.5, 2, 4, 6, 8
Armour stone diameter (m)	D_{n50}	0.0317
Water depth (m)	h	0.600 - 0.825
Incident significant wave height at toe (m)	H_{m0}	0.096 - 0.228
Wave steepness: $s_{m-1,0}=2\pi H_{m0}/gT_{m-1,0}^2$ (-)	$s_{m-1,0}$	0.012 - 0.042
Surf-similarity parameter: $\xi_{m-1,0}=\tan \alpha / s_{m-1,0}^{0.5}$ (-)	$\xi_{m-1,0}$	0.612 - 6.04
Freeboard (m)	R_c	0.075 - 0.30
Non-dimensional freeboard (-)	R_c / H_{m0}	0.33 - 2.08
Non-dimensional width of armour in front of non-protruding crest wall (-)	G_c / H_{m0}	0.44 - 1.04
Non-dimensional stone diameter (-)	D_{n50} / H_{m0}	0.14 - 0.33



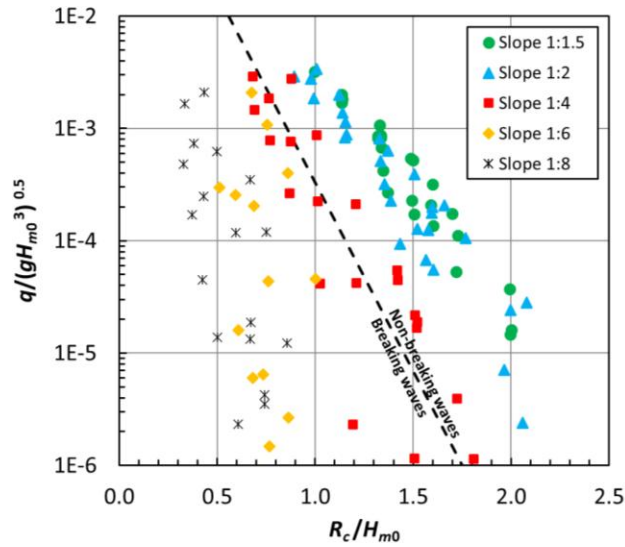
Figure 2: Pictures of wave action on a 1:1.5 slope, 1:2 slope, 1:4 slope and 1:8 slope, respectively.

3.2 Test results

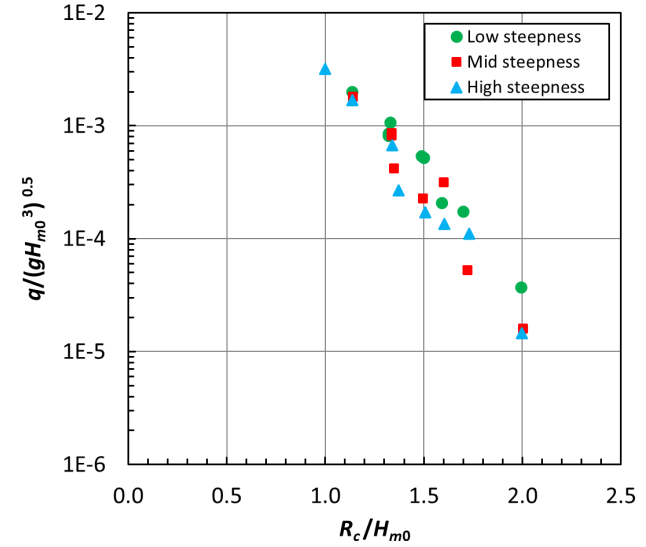
Out of the 120 tests performed, 14 tests led to minor wave overtopping. Here only tests with measured wave non-dimensional overtopping discharges larger than $q^* \geq 1 \cdot 10^{-6}$ were used since smaller values are often less relevant and scale effects may be present. All 106 test results with $q^* \geq 1 \cdot 10^{-6}$ are shown in the upper left panel of Figure 3 with the freeboard (R_c/H_{m0}) at the horizontal axis and the non-dimensional overtopping discharges at the vertical axis.

The results for the various slope angles (various symbols) clearly indicate that there is a dependency on the slope angle; the steeper the slope the larger the mean overtopping discharges. Some waves lead to breaking waves on the slope and other waves to non-breaking waves. In an irregular wave field, not all waves necessarily lead to breaking waves or all to non-breaking waves, but the surf-similarity parameter (or Iribarren number) can be used to distinguish between conditions with “breaking waves” and “non-breaking waves”. A value of the surf-similarity parameter of $\xi_{m-1,0} = 1.8$ can be used as a first estimate with smaller values leading to “breaking waves” and larger values leading to “non-breaking waves”. All tests with 1:1.5 and 1:2 slopes resulted in “non-breaking waves”, all tests with 1:6 and 1:8 slopes resulted in “breaking waves”, while for a 1:4 slope about half of the conditions resulted in “breaking waves” and half in “non-breaking waves”. The dashed line in the upper left panel of Figure 3 indicates the conditions with “breaking waves” on

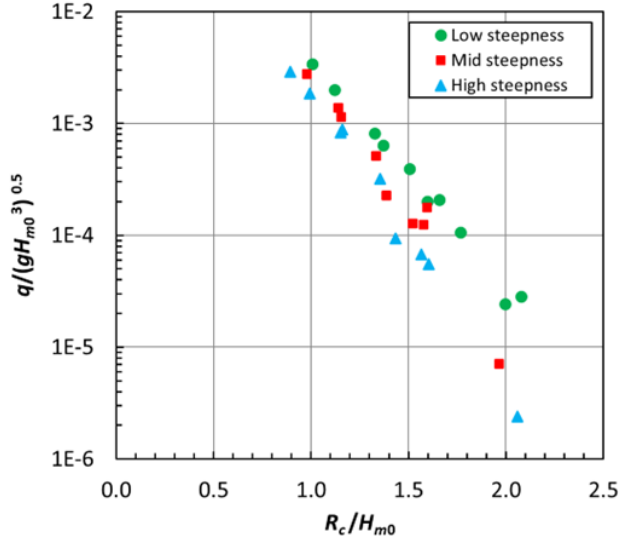
All slopes:



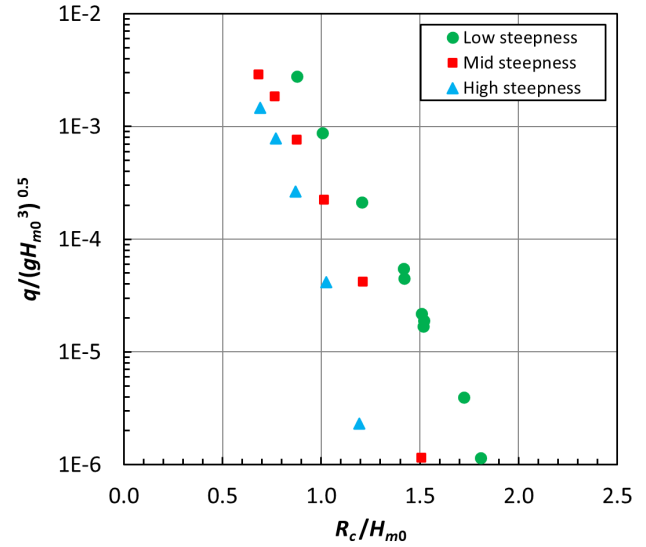
Slope 1:1.5



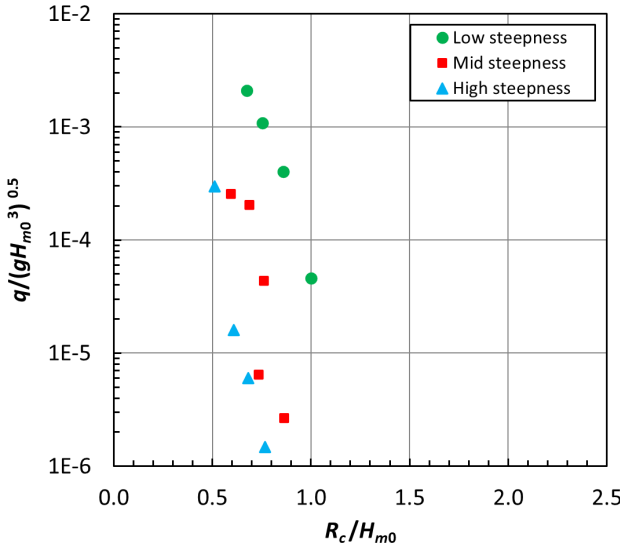
Slope 1:2



Slope 1:4



Slope 1:6



Slope 1:8

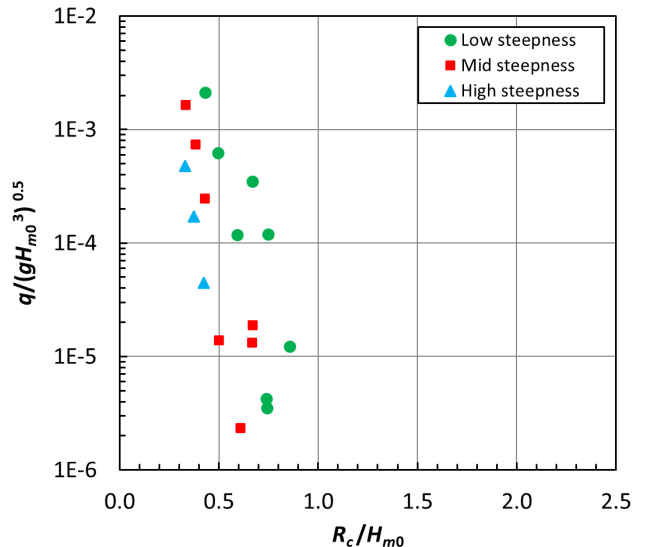


Figure 3: Measured non-dimensional overtopping discharges ($q^* = q/(gH_{m0}^3)^{0.5}$) versus the non-dimensional freeboard (R_c/H_{m0}) for various slopes and various wave steepnesses (for measured discharges larger than $q^* > 1 \cdot 10^{-6}$). Dashed line in upper left panel indicates “breaking waves” on left and “non-breaking waves” on right side of dashed line.

the left side of the dashed line and conditions with “non-breaking waves” on the right side. This figure clearly indicates that the dependency on the slope angle is present for both “breaking waves” and for “non-breaking waves”.

The other five panels of Figure 3 show the test results for each slope angle separately, while the various symbols denote the wave steepness (low steepness: $s_{m-1,0} \leq 0.015$; mid steepness: $0.015 < s_{m-1,0} < 0.03$; high steepness $s_{m-1,0} \geq 0.03$). The dependency on the wave steepness is clearly present but less clear for the steepest 1:1.5 slope (upper right panel) and very clear for the milder slopes 1:4, 1:6 and 1:8. For mild slopes, wave conditions with a low steepness can lead to discharges that are orders of magnitude larger than for conditions with a higher wave steepness. These figures indicate that the dependency on the wave steepness is present for all slopes, although less exposed for the steepest slopes (“non-breaking waves”) and very significant for the mild slopes (“breaking waves”).

Figure 3 illustrates that expressions to estimate wave overtopping discharges need to incorporate effects of the slope angle and wave steepness, both for “breaking waves” and for “non-breaking waves”.

3.3 Analysis of test results

In contrast to Eq.1, Eq.2 contains a dependency on the slope angle and the wave steepness via the surf-similarity parameter. Figure 4 shows the measured non-dimensional discharges as function of the non-dimensional freeboard divided by the surf-similarity parameter $\xi_{m-1,0}$. Figure 4 illustrates that by using the non-dimensional freeboard divided by the surf-similarity parameter $\xi_{m-1,0}$, there still is a dependency on the slope angle, indicating that the dependency of the slope is not sufficiently taken into account via the surf-similarity $\xi_{m-1,0}$ alone. Therefore, Eq.2 needs to be extended. Figure 5 shows the non-dimensional discharges times the slope angle ($q^* \cot \alpha$) versus the non-dimensional freeboard divided by the surf-similarity parameter $\xi_{m-1,0}$ for “breaking waves” and the non-dimensional freeboard divided by the surf-similarity parameter $\xi_{m-1,0}$ to the calibrated power 0.24 for “non-breaking waves”. The left panel of Figure 5 for “breaking waves” and the right panel of Figure 5 for “non-breaking waves” show that the data can be described reasonably well with straight lines in these graphs with logarithmic vertical axes. Calibrating the coefficients of these straight lines based on the present dataset leads to the following expressions:

$$q^* = \frac{q}{\sqrt{gH_{m0}^3}} = 6.8 (\cot^{-1} \alpha) \exp \left[-5.0 \frac{R_c - c_{swell} H_{m0-swell}}{\gamma_f \gamma_b \gamma_v \gamma_\beta \xi_{m-1,0} H_{m0}} \right] \quad (8)$$

with a maximum:

$$q^* = \frac{q}{\sqrt{gH_{m0}^3}} = 0.8 (\cot^{-1} \alpha) \exp \left[-2.5 \frac{R_c - c_{swell} H_{m0-swell}}{\gamma_f \gamma_b \gamma_v \gamma_\beta (\xi_{m-1,0})^{0.24} H_{m0}} \right] \quad (9)$$

where Eq.8 can be seen as the expression for “breaking waves” and Eq.9 as the expression for “non-breaking waves”. Note that the present dataset does not contain conditions with a berm, protruding crest wall, oblique waves, wind, and no swell or infragravity waves in a second wave field ($\gamma_b=1$, $\gamma_v=1$, $\gamma_\beta=1$, $\gamma_w=1$, $H_{m0-swell}=0$). Of the influence factors, only friction is present for which Eq.3 has been used with $c_{f1}=0.7$ and $c_{f2}=0.05$.

The performance of Eqs.8 and 9 is illustrated in Figure 6. The two upper panels show the measured versus the calculated non-dimensional discharges for “breaking waves” (Eq.8), the two middle panels show this comparison for the “non-breaking waves” (Eq.9), while the two lower panels show the combination of both subsets (“breaking” and “non-breaking waves”). The symbols in the left panels indicate the slope angle while the symbols in the right panels indicate the wave steepness. All graphs show that Eqs.8 and 9 describe the data of the present dataset reasonably well. To quantify the performance of Eqs.8 and 9 use is made of the following error measure (for $q^* \geq 1 \cdot 10^{-6}$).

$$\text{RMSLE} = \sqrt{\frac{\sum_{i=1}^{n_{tests}} (\log(Q_{measured}) - \log(Q_{calculated}))^2}{n_{tests}}} \quad (10)$$

The RMSLE value for “breaking waves” is 0.312, for “non-breaking waves” 0.232 and for the total dataset RMSLE=0.267. Here, a RMSLE value lower than 0.4 is considered as a good agreement, a value between 0.4 and 0.5 is considered as a reasonably good agreement and a value larger than 0.5 is considered as a relatively poor agreement.

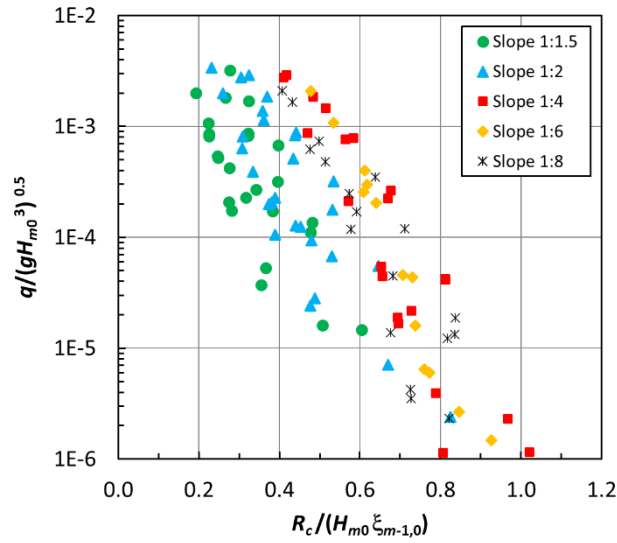
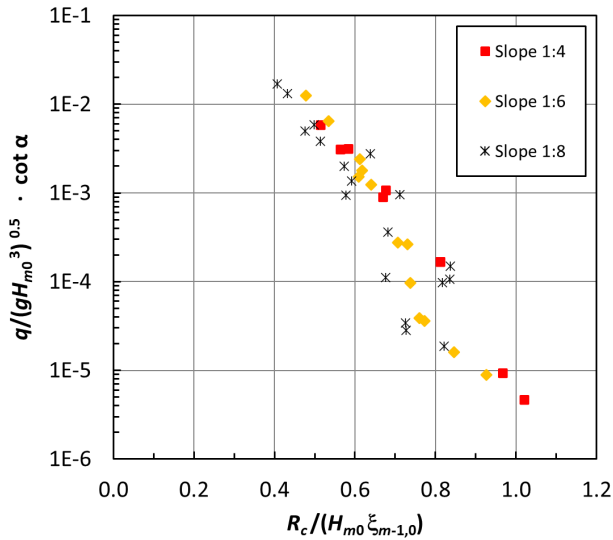


Figure 4: Measured non-dimensional overtopping discharges ($q^* = q/(gH_{m0}^3)^{0.5}$) versus the non-dimensional freeboard (R_c/H_{m0}) divided by the surf-similarity parameter $\xi_{m-1,0}$ ($\xi_{m-1,0} = \tan \alpha / s_{m-1,0}^{0.5}$).

“Breaking waves”:



“Non-breaking waves”:

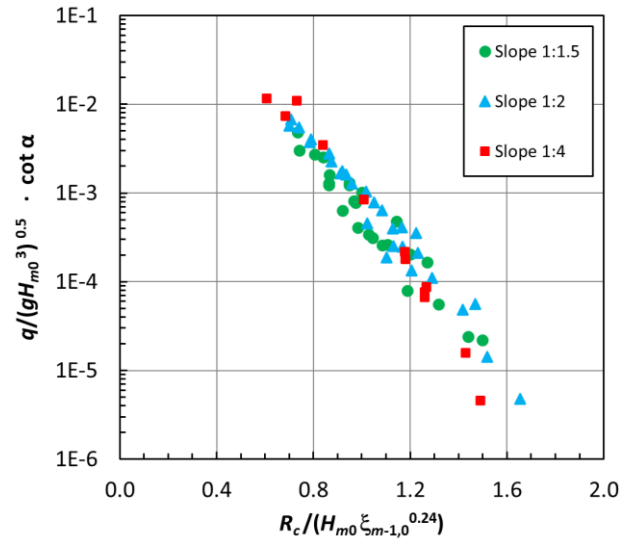


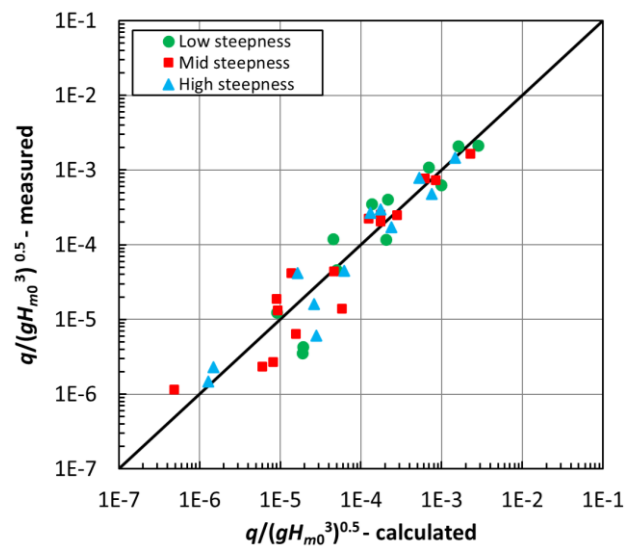
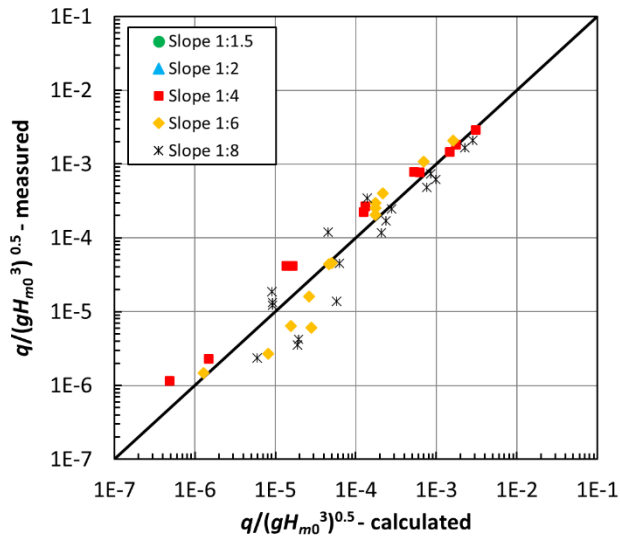
Figure 5: Measured non-dimensional overtopping discharges ($q^* = q/(gH_{m0}^3)^{0.5}$) times the slope angle ($\cot \alpha$) versus the non-dimensional freeboard (R_c/H_{m0}) divided by the surf-similarity parameter $\xi_{m-1,0}$ to the power 1 for “breaking waves” (left panel) and the power 0.24 for “non-breaking waves” (right panel).

3.4 Comparison with other datasets

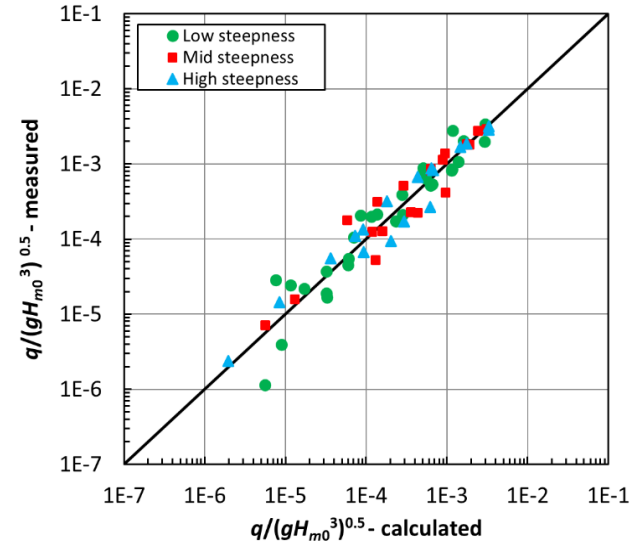
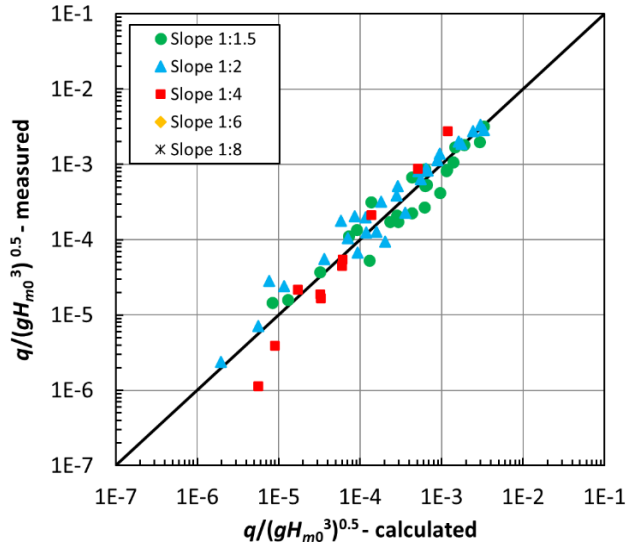
In the new data, the slope angle, wave height, wave steepness, and freeboard were varied. All tested conditions were without wave breaking on the foreshore. To verify the performance of the calibrated expression for conditions with a berm, a protruding crest wall, oblique waves, and conditions including severe wave breaking on the shallow foreshore, use is made of earlier datasets obtained in the same wave flume with similar test set-ups, wave generation, and measurement devices:

- Van Gent *et al.* (2022) with structures including a berm, a crest wall, and a combination of both.
- Van Gent and Van der Werf (2019) with structures with a crest wall under oblique wave attack.
- De Ridder *et al.* (2024) with conditions including severe wave breaking on the foreshore.

“Breaking waves”:



“Non-breaking waves”:



All conditions:

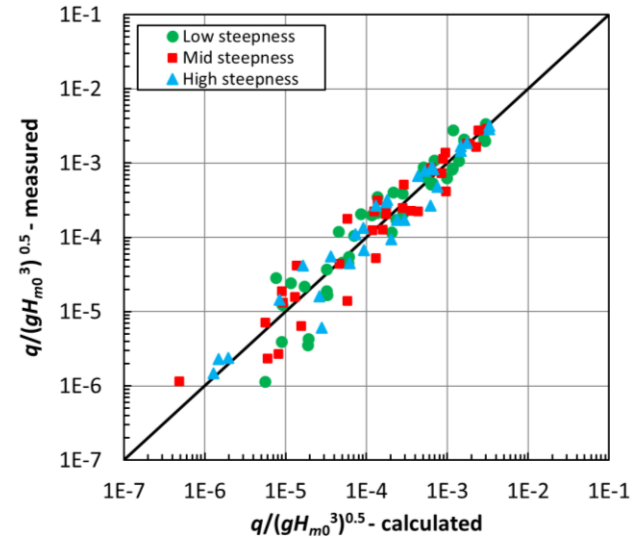
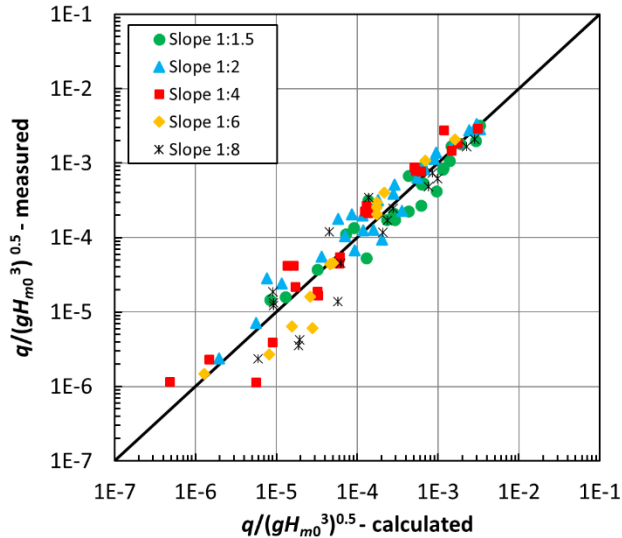


Figure 6: Measured versus calculated overtopping discharges ($q^* = q/(gH_{m0}^3)^{0.5}$) for “breaking waves” (upper panels), “non-breaking waves” (middle panels) and both together (lower panels). Left and right panels refer to the same data but markers refer to either the slope (left panels) or to the wave steepness (right panels).

Since all these earlier tests correspond to conditions that can be considered as “non-breaking conditions”, only Eq.9 in combination with the expressions for influence factors as described in Eqs.3-6 can be evaluated. Note that for the data described in De Ridder *et al.* (2024) severe wave breaking occurs on the foreshore but the surf-similarity parameter (based on the slope of the structure) was always larger than $\xi_{m-1,0} > 1.8$ such that the conditions on the slope of the structure can be considered as “non-breaking waves” on the slope. Table 2 provides the ranges of the relevant parameters, including the new data and the mentioned three earlier datasets.

Table 2: Parameter ranges of the combined dataset.

Parameter	Symbol	Values/Ranges
Seaward slope (-)	$\cot \alpha$	1.5, 2, 4, 6, 8
Wave steepness: $s_{m-1,0} = 2\pi H_{m0} / (gT_{m-1,0}^2)$ (-)	$s_{m-1,0}$	0.006 - 0.046
Surf-similarity parameter: $\xi_{m-1,0} = \tan \alpha / s_{m-1,0}^{0.5}$ (-)	$\xi_{m-1,0}$	0.61 - 19.7
Non-dimensional crest freeboard (-)	R_c / H_{m0}	0.33 - 2.85
Non-dimensional crest level of armour (-)	A_c / H_{m0}	0.33 - 2.85
Non-dimensional width of armour in front of crest wall (-)	G_c / H_{m0}	0 - 1.60
Non-dimensional height of protruding part of crest wall: $(R_c - A_c) / H_{m0}$ (-)	h_c / H_{m0}	0 - 0.75
Non-dimensional berm width (-)	B / H_{m0}	0 - 5.24
Non-dimensional berm level (-)	B_L / H_{m0}	0 - 2.09
Non-dimensional stone diameter (-)	D_{n50} / H_{m0}	0.12 - 0.89
Non-dimensional water depth at toe (-)	h / H_{m0}	0.57 - 11.2
Angle of wave attack (°)	β	0, 15, 30, 45, 60, 75

The data by De Ridder *et al.* (2024) contains conditions with severe wave breaking on the foreshore with a considerable amount of energy in the low-frequencies. Therefore, the wave period at the toe based on the entire wave energy spectrum, can be very long, leading to a very low wave steepness and a high value of the surf-similarity parameter. For large values of the surf-similarity parameter, Bruce *et al.* (2009), EurOtop (2018) and Eldrup *et al.* (2022) proposed an influence factor for friction that reduces the influence of friction for large values of the surf-similarity parameter, in combination with an expression for wave overtopping like Eq.1 without another influence of the wave steepness and structure slope. EurOtop (2018) proposed a reduction of the influence for values larger than $\xi_{m-1,0} > 5$, reaching $\gamma_f = 1$ for $\xi_{m-1,0} = 10$. In the combined dataset values larger than $\xi_{m-1,0} > 5$ only occur in the subset by De Ridder *et al.* (2024). In that dataset the slope was not varied. Here, it is verified whether a friction influence factor that increases for very low wave steepnesses would improve the results using Eq.9 for estimates of the overtopping discharge. That indeed appeared to be the case, but this influence of the wave steepness is much more limited than suggested by, for instance, EurOtop (2018) and Eldrup *et al.* (2022). It is expected that this is partly due to the use of a wave overtopping expression (Eq.9) that already includes influences of the wave steepness and slope. Only for a wave steepness smaller than $s_{m-1,0} < 0.012$ the results improve if a slight increase in the influence factor (lower influence of friction) is accounted for. For values smaller than $s_{m-1,0} < 0.012$, the influence factor for friction obtained from Eq.3 can be modified as proposed here:

$$\gamma_{f-low\ steepness} = \gamma_f + 12 (0.012 - s_{m-1,0}) (1 - \gamma_f) \quad (11)$$

for $0.0006 < s_{m-1,0} < 0.012$ while γ_f is calculated using Eq.3. Figure 7 illustrates this expression for a situation in which Eq.3 would yield $\gamma_f = 0.4$. Whether this expression can also be applied to other structure slopes still needs to be verified.

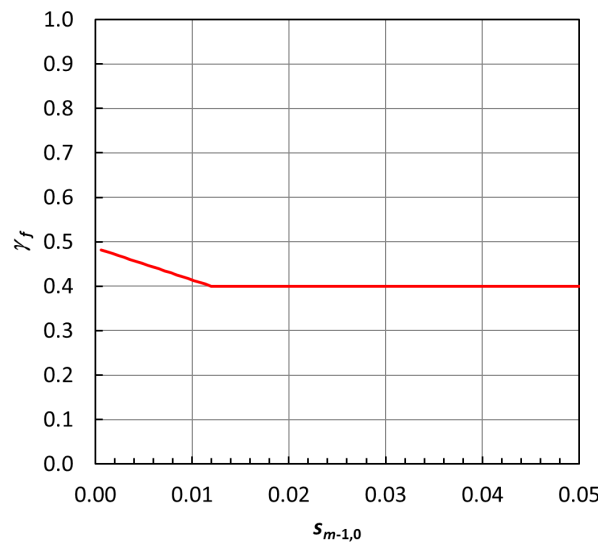


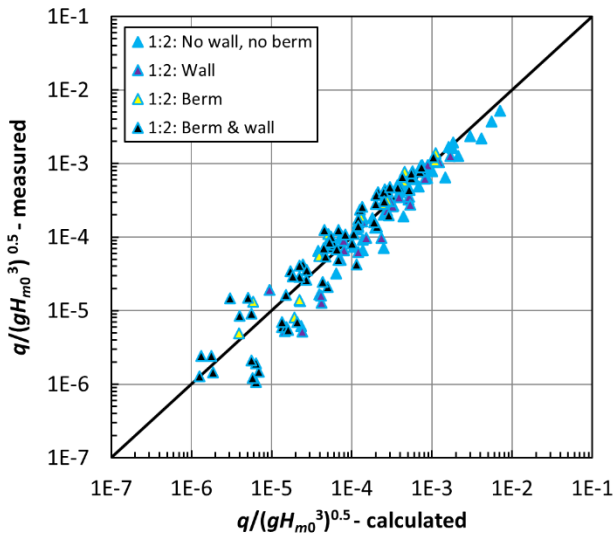
Figure 7: Dependency of the influence factor for friction (γ_f) on the wave steepness ($s_{m-1,0}$).

First, the data (152 tests with $q^* \geq 1 \cdot 10^{-6}$; “non-breaking waves”) by Van Gent *et al.* (2022) is compared to the new expressions (Eq.9 with Eqs.3-6). The tested structures consisted of straight 1:2 rock-armoured slopes, 1:2 slopes with a statically stable horizontal berm with various widths and various berm levels, structures with protruding crest walls, and structures with a combination of a berm and a protruding crest wall. The upper left panel of Figure 8 shows the comparison with the mentioned set of expressions. The match between the data and the set of expressions is good (RMSLE=0.285) and the match is comparable to the accuracy for the data described in Section 3.2 (RMSLE=0.267).

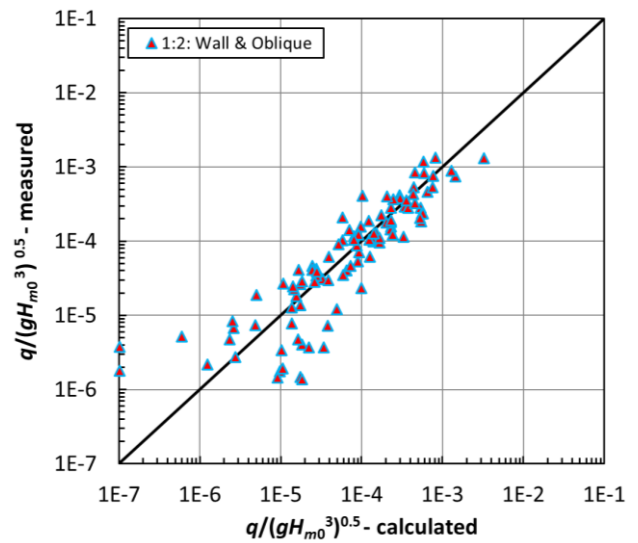
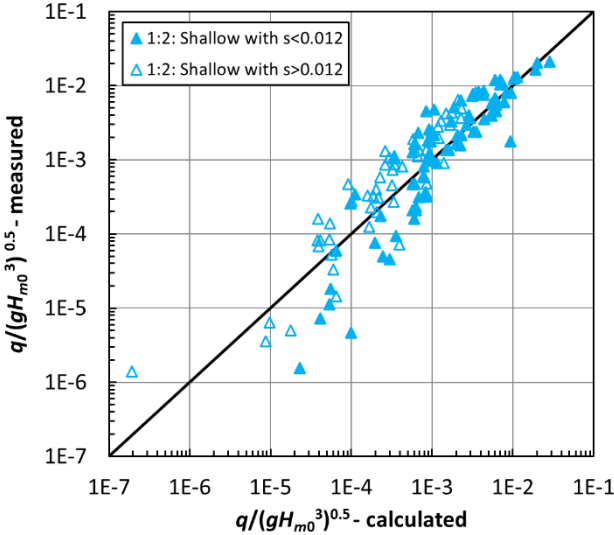
Secondly, the data (101 tests with $q^* \geq 1 \cdot 10^{-6}$; “non-breaking waves”) by Van Gent and Van der Werf (2019) is compared to the new expressions (Eq.9 with Eqs.3-6). The tested structures consisted of a straight 1:2 rock-armoured slope with a protruding crest wall. The angle of wave attack was varied between perpendicular ($\beta=0^\circ$), in steps of 15° , to very oblique waves ($\beta=75^\circ$). Eq.6 was based on these tests, and this expression is considered valid only for conditions without severe wave breaking on the foreshore. The upper right panel of Figure 8 shows the comparison with the new set of expressions. The match between the data and the set of expressions is reasonably good (RMSLE=0.451).

Thirdly, the data (133 tests with $q^* \geq 1 \cdot 10^{-6}$; “non-breaking waves”) by De Ridder *et al.* (2024) is compared to the new expressions (Eq.9 with Eqs.3-6). The tested structures consisted of a straight 1:2 rock-armoured slope with a non-protruding crest wall. In contrast to the other subsets with a horizontal foreshore without wave breaking before the waves reach the structure, these tests included conditions with severe wave breaking on the tested sloping foreshores (1:20, 1:50 and 1:100 slopes). De Ridder *et al.* (2024) evaluated a large number of expressions and concluded that an expression including the wave steepness based on wave parameters excluding the low frequencies, provides accurate results, although an expression with the wave steepness based on the entire wave energy spectrum only performs slightly less (Eq. 23 versus Eq. 24 in De Ridder *et al.*, 2024). Here, the wave steepness $s_{m-1,0}$ is based on the entire wave energy spectrum. The optimal power of the wave steepness in the wave overtopping expression was 0.12 in Eq.23 of De Ridder *et al.* (2024). This corresponds to the optimal power for the new data (Eq.8) where the optimal power for the surf-similarity parameter for non-breaking waves is -0.24 (in the surf-similarity parameter, the wave steepness is raised to the power -0.5). Here, Eq.11 is used for those tests with a wave steepness lower than $s_{m-1,0} < 0.012$. The lower right panel of Figure 8 shows the comparison with the new set of expressions, with filled symbols for tests with $s_{m-1,0} < 0.012$ and open symbols for tests with $s_{m-1,0} > 0.012$. The match between the data and the set of expressions is good (RMSLE=0.392). If the dependency of the friction on the wave steepness, as shown in Eq.11 and Figure 7 would not be used, the match would be clearly less (RMSLE=0.504).

The lower right panel of Figure 8 shows the data of all four subsets together. The match between the data and Eqs.8 and 9 with influence factors in Eqs.3-6 and Eq.11 (492 tests with $q^* \geq 1 \cdot 10^{-6}$) is good (RMSLE=0.352). The dashed line in the lower right panel of Figure 8 shows an expression for a design including safety (5% of all tests are above the dashed line), as will be discussed in the next section.

Van Gent *et al.* (2022): Berms and crest walls


Van Gent and Van der Werf (2019): Oblique waves


De Ridder *et al.* (2024): Shallow water


All:

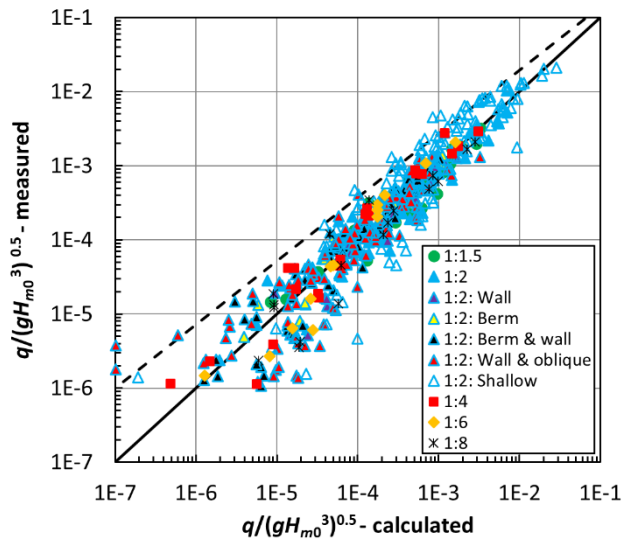


Figure 8: Measured versus calculated overtopping discharges ($q^* = q/(gH_{m0}^3)^{0.5}$) for various datasets, including structures with a crest wall, with a berm, with shallow water conditions, and with oblique wave attack. Solid lines denote perfect agreement using Eqs. 8 and 9. Dashed line in lower right graph denotes expression for design purposes (Eq. B8).

4 Discussion

The comparison between the test results and the empirical expressions as described in the previous section shows a rather good agreement between both. However, two sources of potential underestimates of actual wave overtopping discharges using the derived expressions are discussed here: *a)* White spots in the applied dataset, and *b)* Applications outside the range of the dataset.

The variations of each of the relevant parameters in the applied dataset is quite extensive, but that does not mean that all relevant combinations of parameters are well covered by the dataset. For a 1:2 slope (which is a very common slope for rock-armoured structures) a large range of configurations with various berms and various protruding crest walls was tested, as well as a wide range of angles of wave attack, but this was not done for the other slopes. The parameter ranges are quite well covered for “non-breaking waves”, but for “breaking waves” there are a number of combinations of parameters missing in the dataset. For instance, the dataset does not contain tests with mild slopes such as 1:8 and 1:6 slopes with berms. Thus, the data does not cover all combinations, such that some combinations are well represented in the dataset and other combinations are not. The latter are so-called white spots in the dataset. Due to the presence of white

Wave overtopping discharges at rubble mound breakwaters:

$$q^* = \frac{q}{\sqrt{gH_{m0}^3}} = 6.8 (\cot^{-1} \alpha) \exp \left[-5.0 \frac{R_c - 0.4 H_{m0-swell}}{\gamma_f \gamma_b \gamma_v \gamma_\beta \xi_{m-1,0} H_{m0}} \right] \quad (B1)$$

(breaking waves)

with a maximum of:

$$q^* = \frac{q}{\sqrt{gH_{m0}^3}} = 0.8 (\cot^{-1} \alpha) \exp \left[-2.5 \frac{R_c - 0.4 H_{m0-swell}}{\gamma_f \gamma_b \gamma_v \gamma_\beta (\xi_{m-1,0})^{0.24} H_{m0}} \right] \quad (B2)$$

(non-breaking waves)

with influence factors for

Friction: $\gamma_f = \gamma_{f1} = 1 - 0.7 \left(\frac{D_{n50}}{H_{m0}} \right)^{0.05}$ **for $s_{m-1,0} \geq 0.012$** (B3a)

$\gamma_f = \gamma_{f2} = \gamma_{f1} + 12 (0.012 - s_{m-1,0}) (1 - \gamma_{f1})$ **for $0.0006 < s_{m-1,0} < 0.012$** (B3b)

Berm: $\gamma_b = 1 - 18 \left(\frac{s_{m-1,0} B}{H_{m0}} \right)^{1.3} \left(1 - 0.34 \left(\frac{B_L}{s_{m-1,0} A_c} \right)^{0.2} \right)$ **for $\cot \alpha \leq 4$** (B4)

Protruding crest wall: $\gamma_v = 1 + 0.45 \left(\frac{R_c - A_c}{R_c} \right)$ **for $\cot \alpha \leq 4$** (B5a)

$\gamma_v = 1 + 0.1125 \cot \alpha \left(\frac{R_c - A_c}{R_c} \right)$ **for $\cot \alpha \geq 4$** (B5b)

Oblique waves: $\gamma_\beta = 0.65 \cos^2 \beta + 0.35$ **for $H_{m0-deep} / h_{toe} < 1$** (B6)

Accounting for the influence of wind on wave overtopping for structures with a protruding crest wall:

Overtopping with wind: $q_w = \gamma_w q$ **with** $\gamma_w = 1 + 0.075 \frac{h_c}{H_{m0}} (q^*)^{-0.3}$ (B7)

For design purposes (95% confidence level):

$q_{design} = (q^*)^{0.857}$ **with q^* using Eqs. B1 to B7** (B8)

Box 1: Overview of empirical expressions to estimate wave overtopping discharges at rubble mound breakwaters with a permeable core ($1 \cdot 10^{-6} \leq q^* \leq 1 \cdot 10^{-1}$).

spots in the dataset, for some configurations or wave loading special attention is required, especially if derived expressions may lead to important underestimates of the wave overtopping discharges. A second reason to be careful with applications of the derived expressions are applications for structure types that have not been analyzed here. Three important limitations are mentioned here. The first two are related to white spots in the dataset and the third is related to applications outside the ranges of the tests:

- *Oblique waves in combination with a shallow foreshore.* All test conditions in the dataset with oblique waves were without wave breaking on the foreshore. Oblique wave attack generally leads to a reduction in wave overtopping. However, to what extent that reduction is valid in case of breaking waves on a shallow foreshore remains unknown. For instance, breaking waves that propagate in increasingly shallow water along rubble mound breakwaters under a large angle (for instance $\beta > 70^\circ$) lead to quite a different wave interaction with the structure than if these waves are not breaking before they reach the structure. Shallow water with severe wave breaking can be characterized by the ratio between the deep-water wave height ($H_{m0-deep}$) and the depth at the toe of the structure (h_{toe}): $H_{m0-deep} / h_{toe} \geq 1$ (see Van Gent, 1999, and De Ridder *et al.*, 2024). For conditions with severe wave breaking on the shallow foreshore, it is recommended not to apply a reduction factor due to oblique waves ($\gamma_\beta = 1$) until systematic data and adequate guidelines for such conditions become available.

- *Mild slopes in combination with berm and/or protruding crest wall.* All test conditions in the dataset with mild slopes (1:8 and 1:6) were for configurations without a berm and without a protruding crest wall. Adding a berm to such a mild slope may effectively lead to an average slope that is outside the range of the tests (milder than 1:8); it remains unclear whether this could lead to an overestimate of the discharge. A protruding crest wall could be somewhat less effective in redirecting the run-up tongue in the upward or seaward direction than a protruding crest wall on a structure with a steeper slope. For conditions with a slope that is milder than 1:4, it is advised not to apply a reduction factor due to a berm (for $\cot \alpha \geq 4$, $\gamma_b = 1$) until systematic data and adequate guidelines for such conditions become available. For conditions with a slope that is milder than 1:4, it is advised to apply a coefficient in the influence factor for protruding crest walls that is larger than $c_v = 0.45$ in Eq. 5: $c_v = 0.1125 \cdot \cot \alpha$ for $\cot \alpha \geq 4$, until systematic data and adequate guidelines for such conditions become available.
- *Impermeable core.* All structures in the applied dataset had a permeable core. If the core would be impermeable (in practice for instance a revetment with a core of sand), the wave run-up and wave overtopping can be larger than for such a structure with a permeable core. Therefore, the set of expressions may lead to underestimates of the overtopping discharges for structures with an impermeable core. For estimates of wave overtopping discharges at rock-armoured slopes with an impermeable core, reference is made to Koosheh *et al.* (2022). For estimates of wave overtopping discharges at rock-armoured slopes with a permeable core as tested here, the derived expressions are considered valid. However, numerical modelling by Irías Mata and Van Gent (2023) and Castiglione *et al.* (2023) indicate that for permeable structures with a relatively low permeability (non-standard), wave overtopping discharges can increase up to a factor two to three.

Besides configurations or conditions that require special attention due to potential underestimates of the overtopping discharges, there are also some configurations or conditions for which the set of expressions can lead to overestimates of the overtopping discharges. There are indications that oblique waves in combination with a berm in the seaward slope leads to a somewhat larger reduction in the discharges than the expressions suggest; the berm is more effective for oblique waves (see also Van Gent, 2022).

Effects of wind on water levels and the wave conditions at the toe need to be taken into account in the conditions that are used in the expressions for wave overtopping. Other effects of the wind are small or negligible, except for structures with a protruding crest wall. A protruding crest wall can direct the flow in an upward direction such that the water above the tip of the protruding crest wall becomes susceptible to wind. The expression referred to here (Eq. 7) has been developed for perpendicular wave attack. For oblique wave attack the potential influence of onshore wind on wave overtopping discharges is less than for perpendicular wave attack. Thus, using Eq. 7 may lead to overestimates of the wave overtopping discharges for oblique wave attack at structures with a protruding crest wall.

Taking above considerations into account leads to the set of expressions shown in Box 1. Note that these expressions provide estimates of wave overtopping but do not contain a safety margin that is likely to be required for the actual design. The error measure RMLSE=0.352 (Eqs. B1 to B7) based on the applied dataset can be used in probabilistic design methods. For design purposes a 95% confidence level or 5%-exceedance level (*i.e.* 95% of the tests provide a lower discharge) can be used: $q_{design}^* = (q^*)^{0.857}$ where q^* is obtained using Eqs. B1 to B7 shown in Box 1. Note that since q^* is smaller than one, the power (0.857) smaller than one leads to an increase of the design value q_{design}^* compared to the best estimate value q^* . The dashed line in the lower right panel of Figure 8 shows the expression (Eq. B8) for a design including safety. The graph shows that for only a few tests (5% of all tests), the measured values are larger than the values calculated with the expression for the design (dashed line).

5 Conclusions and recommendations

Mean wave overtopping discharges at rubble mound structures were measured for various rock-armoured slopes. In the physical model tests the structure slope was varied between 1: 1.5 and 1:8. The wave overtopping discharges appeared to be dependent on the slope ($\cot \alpha$) for both “breaking waves” and “non-breaking waves” on the slope. Existing expressions that also account for friction, a berm (if present), a protruding crest wall (if present), and the angle of wave attack, were extended by incorporating both the slope angle and the wave steepness of the incident waves at the toe. The derived empirical equations are summarized in Box 1. The match between the empirical equations and the new data (Figure 6) and the match between the expressions and data from earlier tests (Figure 8) is good. The equations in Box 1

can be used to estimate wave overtopping discharges for rubble mound structures with a permeable core. For design purposes, the uncertainty in the estimates needs to be accounted for by using a safety factor or by using a probabilistic method.

The applied dataset has some limitations that require special attention for conditions that are not well represented in the dataset. This includes situations with obliquely incident waves in combination with severe wave breaking on the foreshore. It is recommended to study wave overtopping for such conditions with new systematic physical model tests. Although not often applied in practice, mild slopes (slopes more gentle than 1:4) in combination with a berm in the seaward slope, or in combination with a protruding crest wall, require further attention. Additional physical model tests for such conditions are also recommended.

The guidelines to estimate wave overtopping discharges as presented here perform much better than existing guidelines since most existing guidelines for rubble mound breakwaters ignore the explicit influence of the structure slope and the wave steepness (*e.g.* EurOtop, 2018, Eq.5.6). Both for “breaking waves” and for “non-breaking waves” the slope and the wave steepness clearly affect wave overtopping discharges, and therefore expressions that ignore these effects should not be used if accurate estimates are required (see also upper left panel of Figure 3).

It is recommended to use the obtained data to extend prediction methods for wave overtopping discharges based on machine learning techniques such as described in Den Bieman *et al.* (2021). The data and prediction method can also be applied to validate numerical models that simulate wave overtopping.

The present study was focused on wave overtopping discharges. In addition to mean wave overtopping discharges also wave overtopping volumes, velocities, and flow depths in wave overtopping events are also of interest. It is recommended to analyse the influence of the studied parameters such as slope angle and wave steepness, also for individual overtopping events.

Acknowledgements

Daan Jumelet (DEME group) is acknowledged for participating in the supervision of the new tests (Sections 3.1 and 3.2). Dennis van Kester (Van Oord) and Menno de Ridder (Deltares) are acknowledged for reviewing an earlier version of this paper. The assistance during the physical model tests by Wesley Stet, Danny van Doeveren and Peter Alberts is highly appreciated.

Funding

This study was realized with the support by a TKI (Top Consortia for Knowledge and Innovation) subsidy (Delta Technology project CLIMACS, project DEL171), the ‘Vereniging van Waterbouwers’, and by the Deltares’ Strategic Research Program Resilient Infrastructure (MS5.5).

Author contributions (CRediT)

MvG: Conceptualisation, Investigation, Formal analysis, Validation, Visualisation, Writing-original draft, Funding acquisition; JvM: Investigation, Writing-Reviewing & editing; PMN: Writing-Reviewing & editing.

Data access statement

The new data is available upon request (license CC-BY-NC-SA).

Declaration of interests

The authors report no conflict of interest.

Notation

Name	Symbol	Unit
slope angle of structure	α	°
angle of wave attack ($\beta=0^\circ$ for perpendicular wave attack)	β	°
influence factor for wave overtopping	γ	-
crest level of armour at crest, relative to still water level	A_c	m
berm width	B	m
berm level: the vertical distance of the berm relative to the crest of the armour A_c	B_L	m
stone diameter	D_{n50}	m
width of the crest armour (seaward of crest wall)	G_c	m
gravitational acceleration	g	m/s ²
significant wave height of incident waves at toe of structures, based on wave energy spectrum	H_{m0}	m
significant wave height of swell or infragravity waves in case of a second wave field	$H_{m0\text{-swell}}$	m
water depth	h	m
protruding part of a crest wall ($h_c = R_c - A_c$)	h_c	m
mean overtopping discharge	q	m ³ /s/m
non-dimensional mean overtopping discharge	q^*	-
crest freeboard (crest height relative to still water level; negative for submerged structures)	R_c	m
wave steepness calculated using $s_{m-1,0} = 2\pi H_{m0} / (gT_{m-1,0}^2)$	$s_{m-1,0}$	-
spectral mean wave period of the incident waves	$T_{m-1,0}$	s

References

- Battjes, J.A. (1974): Computation of set-up, longshore currents, run-up and overtopping due to wind-generated waves, Ph.D.-thesis, Delft University of Technology, Delft.
- Bruce, T., J.W. van der Meer, L. Franco, J.M. Pearson (2009): Overtopping performance of different armour units for rubble mound breakwaters, Elsevier, Coastal Engineering, <https://doi.org/10.1016/j.coastaleng.2008.03.015>
- Castiglione, F., M. Stagnitti, R.E. Musumeci, E. Foti (2023): Influence of Van Gent parameters on the overtopping discharge of a rubble mound breakwater, J. Mar. Sci. Eng. 2023, 11(8), 1600, <https://doi.org/10.3390/jmse11081600>
- Chen, W., J.J. Warmink, M.R.A. van Gent, S.J.M.H. Hulscher (2021): Numerical modelling of wave overtopping at dikes using OpenFOAM®, Elsevier, Coastal Engineering, <https://doi.org/10.1016/j.coastaleng.2021.103890>
- Chen, W., J.J. Warmink, M.R.A. van Gent, S.J.M.H. Hulscher (2022): Numerical investigation of the effects of roughness, a berm and oblique waves on wave overtopping processes at dikes, Elsevier, Applied Ocean Research, 118, <https://doi.org/10.1016/j.apor.2021.102971>
- Dekker, J., S. Caires, M.R.A. van Gent (2007): Reflection of non-standard wave energy spectra by sloping structures, World Scientific, Proc. Coastal Structures 2007, 760-770.
- Den Bieman, J.P., M.R.A. van Gent, H.F.P. van den Boogaard (2021): Wave overtopping predictions using an advanced machine learning technique, Elsevier, Coastal Engineering, <https://doi.org/10.1016/j.coastaleng.2020.103830>
- De Ridder, M.P., J. Kramer, J.P. den Bieman, I. Wenneker (2023): Validation and practical application of nonlinear wave decomposition methods for irregular waves, Elsevier, Coastal Engineering, <https://doi.org/10.1016/j.coastaleng.2023.104311>

- De Ridder, M.P., D.C.P. van Kester, R. van Bentem, D.Y.Y. Teng, M.R.A. van Gent (2024): Wave overtopping discharges at rubble mound structures in shallow water, Elsevier, Coastal Engineering, <https://doi.org/10.1016/j.coastaleng.2024.104626>
- De Ridder, M.P., D.C.P. van Kester, P. Mares-Nasarre, M.R.A. van Gent (2025): Individual overtopping volumes, water layer thickness and front velocities at rubble mound breakwaters with a smooth crest in shallow water, Elsevier, Coastal Engineering, <https://doi.org/10.1016/j.coastaleng.2025.104701>
- Eldrup, M.R. and T. Lykke Andersen (2018): Recalibration of overtopping roughness factors of different armour types, Thomas Telford, Proc. Coasts, Marine Structures and Breakwaters 2017, Liverpool, 1011-1020, <https://doi.org/10.1680/cmsb.63174.1011>
- Eldrup, M.R., T. Lykke Andersen, K. van Doorslaer, J.W. van der Meer (2022): Improved guidance on roughness and crest width in overtopping of rubble mound structures along EurOtop, Elsevier, Coastal Engineering, <https://doi.org/10.1016/j.coastaleng.2022.104152>
- EurOtop (2018): Manual on wave overtopping of sea defences and related structures, J.W. van der Meer, N.W.H. Allsop, T. Bruce, J. de Rouck, A. Kortenhaus, T. Pullen, H. Schüttrumpf, P. Troch, B. Zanuttigh (Eds.), www.overtopping-manual.com (incl. Errata November 2019).
- Gallach-Sánchez, D. (2018): Experimental study of wave overtopping performance of steep low-crested structures, Ph.D. Thesis, Universiteit Gent, Belgium.
- Gallach-Sánchez, D., P. Troch, A. Kortenhaus (2021): A new average wave overtopping prediction formula with improved accuracy for smooth steep low crested structures, Elsevier, Coastal Engineering, <https://doi.org/10.1016/j.coastaleng.2020.103800>
- Goda Y. (1971): Expected rate of irregular wave overtopping of seawalls, Coastal Engineering in Japan, 14, 45-51, JSCE, Tokyo.
- Iriás Mata, M. and M.R.A. van Gent (2023): Numerical modelling of wave overtopping discharges at rubble mound breakwaters using OpenFOAM®, Elsevier, Coastal Engineering, <https://doi.org/10.1016/j.coastaleng.2022.104274>
- Jin Y., W. Wang, C. Pákozdi, A. Kamath, H. Bihs (2022): Numerical Investigation on Wave Overtopping at a Double-dike Defence Structure in Response to Climate Change Induced Sea Level Rise, MDPI, Fluids, <https://doi.org/10.3390/fluids7090295>
- Koosheh, A., A. Etemad-Shahidi, N. Cartwright, R. Tomlinson, M.R.A. van Gent (2022): Experimental study of wave overtopping at rubble mound seawalls, Elsevier, Coastal Engineering, <https://doi.org/10.1016/j.coastaleng.2021.104062>
- Lioutas, A.C., G.M. Smith, H.J. Verhagen (2012): Spatial distribution of overtopping, Proc. ICCE, <https://doi.org/10.9753/icce.v33.structures.63>
- Medina, J.R. and J. Molines (2016): Roughness factor in overtopping estimation, Proc. ICCE 2016, <http://dx.doi.org/10.9753/icce.v35.structures.7>
- Molines, J. and J.R. Medina (2015): Calibration of overtopping roughness factors for concrete armor units in non-breaking conditions using the CLASH database, Elsevier, Coastal Engineering, <https://doi.org/10.1016/j.coastaleng.2014.11.008>
- Owen, M.W. (1980): Design of seawalls allowing for wave overtopping (Report No. Ex 924). Hydraul. Res. HR Wallingford.
- Pepi, Y., A. Romano, L. Franco (2022): Wave overtopping at rubble mound breakwaters: A new method to estimate roughness factor for rock armours under non-breaking waves, Elsevier, Coastal Engineering, <https://doi.org/10.1016/j.coastaleng.2022.104197>
- Stagnitti M., J.L. Lara, R.E. Musumeci, E. Foti (2023): Numerical modeling of wave overtopping of damaged and upgraded rubble-mound breakwaters, Elsevier, Ocean Engineering, <https://doi.org/10.1016/j.oceaneng.2023.114798>
- TAW (2002): Technical Report Wave Run-up and Wave Overtopping at Dikes, Technical Advisory Committee on Flood Defence (TAW), Delft.
- Van der Werf, I.M. and M.R.A. van Gent (2018): Wave overtopping over coastal structures with oblique wind and swell waves, J. Mar. Sci. Eng. 2018, 6 (4), 149, <https://doi.org/10.3390/jmse6040149>.
- Van Gent, M.R.A. (1999): Physical model investigations on coastal structures with shallow foreshores; 2D model tests with single and double-peaked wave energy spectra, Delft Hydraulics Report H3608, December 1999, Delft, <http://dx.doi.org/10.13140/RG.2.2.17091.68644>

- Van Gent, M.R.A. (2001): Wave run-up on dikes with shallow foreshores, *Journal of Waterway, Port, Coastal and Ocean Engineering*, ASCE, 127-5, Sept/Oct 2001, 254-262, [https://doi.org/10.1061/\(ASCE\)0733-950X\(2001\)127:5\(254\)](https://doi.org/10.1061/(ASCE)0733-950X(2001)127:5(254))
- Van Gent, M.R.A., and I.M. van der Werf (2019): Influence of oblique wave attack on wave overtopping and wave forces on rubble mound breakwater crest walls, Elsevier, *Coastal Engineering*, <https://doi.org/10.1016/j.coastaleng.2019.04.001>
- Van Gent, M.R.A., G. Wolters, A. Capel (2022): Wave overtopping discharges at rubble mound breakwaters including effects of a crest wall and a berm, Elsevier, *Coastal Engineering*, <https://doi.org/10.1016/j.coastaleng.2022.104151>
- Van Gent, M.R.A. (2022): Wave overtopping at dikes and breakwaters under oblique wave attack, ASCE, Proc. ICCE 2022, Sydney, <https://doi.org/10.9753/icce.v37.papers.5>
- Van Gent, M.R.A., R.J. van der Bijl, S.J. Dijkstra, L.F. van Vliet, D. Wüthrich (2024): Wind effects on wave overtopping discharges at dikes and breakwaters with a crest wall, ASCE, Proc. ICCE 2024, Rome, <https://doi.org/10.9753/icce.v38.papers.6>
- Van Marrewijk, J. (2024): Influence of the slope angle on wave overtopping at rubble mound breakwaters, M.Sc. thesis, Delft University of Technology, Delft.
- Vieira Leite, J.P., J.W. van der Meer, L. Franco, A. Romano, Y. Pepi, T. Bruce, L. Vieira Pinheiro, M. Menendez (2019): Distribution of overtopping wave volumes caused by crossing seas, Proc. Coastal Structures 2019, Hannover.
- Zelt, J.A. and J.E. Skjelbreia (1992): Estimating incident waves and reflected wave fields using an arbitrary number of wave gauges, Proc. ICCE 1992, Venice, <https://doi.org/10.1061/9780872629332.058>